

Triazabicyclodecene Guanidine as Efficient and Reusable Solid Catalyst for the Addition of Nitromethane to Cyclo Pentenone

Samaila Muazu Batagarawa* and Ahmed Lawal Mashi

Corresponding authors: Samaila Muazu Batagarawa

¹Department of Pure and Industrial Chemistry, Umaru Musa Yaradua University, P.M. B 2218, Katsina, Nigeria.

Abstract

Silica from Rice husk ash (RHA) was extracted and functionalized with 1, 5, 7-triazabicyclo [4.4.0] dec-5-ene (TBD) guanidine. The catalyst was prepared, first by the reaction of 3-(chloropropyl)triethoxy silane (CPTES) with silica at room temperature and pressure to form chloro propyl silica material (RHACCl). It was later grafted with TBD guanidine at refluxing temperature of 110 °C to form the solid catalyst (RHAPrTBD). Thermogravimetric analysis showed the number of active pendant groups in the catalyst was 1.20 mmol g⁻¹ with a surface area of 326 m²g⁻¹. Both FT IR, ¹³C and ²⁹Si NMR data were in agreement with the proposed structure. The material was used to catalyse the addition of nitromethane to cyclopentenone. The result showed 90% conversion after 4h reaction time with good selectivity for nitromethylcyclopentanone. The catalyst was recovered and reused 5 more times, maintaining almost 72 % of its catalytic activity.

Keywords: triazabicyclodecene, silica-guanidine, nanoparticles, pendant group, Nitromethane, cyclopentanone,

Date of Submission: 26-02-2020

Date of Acceptance: 09-03-2020

I. Introduction

As strong organic bases, guanidines catalyse various types of organic reactions. Among the guanidine compounds, 1,1,3,3-tetramethylguanidine (or N,N,N-tetramethylguanidine, (TMG) is regarded as a typical and fundamental guanidine compound, and it has been utilised in many kinds of base-catalysed reactions. Another example, is the preparation of pentaalkylguanidines by Barton et al., (1982) and their application in organic synthesis as sterically-hindered organic bases, which are called 'Barton's bases'. Similarly, bicyclic guanidines, such as 1,5,7-triazabicyclo(4.4.0)dec-5-ene (TBD) and its *N*-methyl analogue (MTBD) were introduced by Schwesinger, (1985). One of the derivatives of guanidine, which is referred to as arginine, is found in the side-chain of the amino acid, and plays an important role in the interaction with enzymes or receptors through hydrogen bonding and/or electrostatic interactions, largely because of its strong basic character (de Assuncao, et al., 2010).

Guanidines have been used both as homogeneous and heterogeneous catalysts in several base catalyzed organic reactions, such as Michael addition (Ye, et al., 2005; Ma and Cheng, 1999), transesterification of vegetable oils (Schuchardt, et al., 1998; Serchelli, et al., 1999; Faria, et al., 2008; Meloni, et al., 2011), methylation of phenol (Bercelo, et al., 1990), Aldol and Knoevenagel condensation reactions (Serchelli, et al., 1997), esterification of glycerol (Jerome, 2004) and in cyclo addition of carbon dioxide to cyclic carbonates (Zhang, et al., 2006; Barbarini, et al., 2003; Dai, et al., 2009).

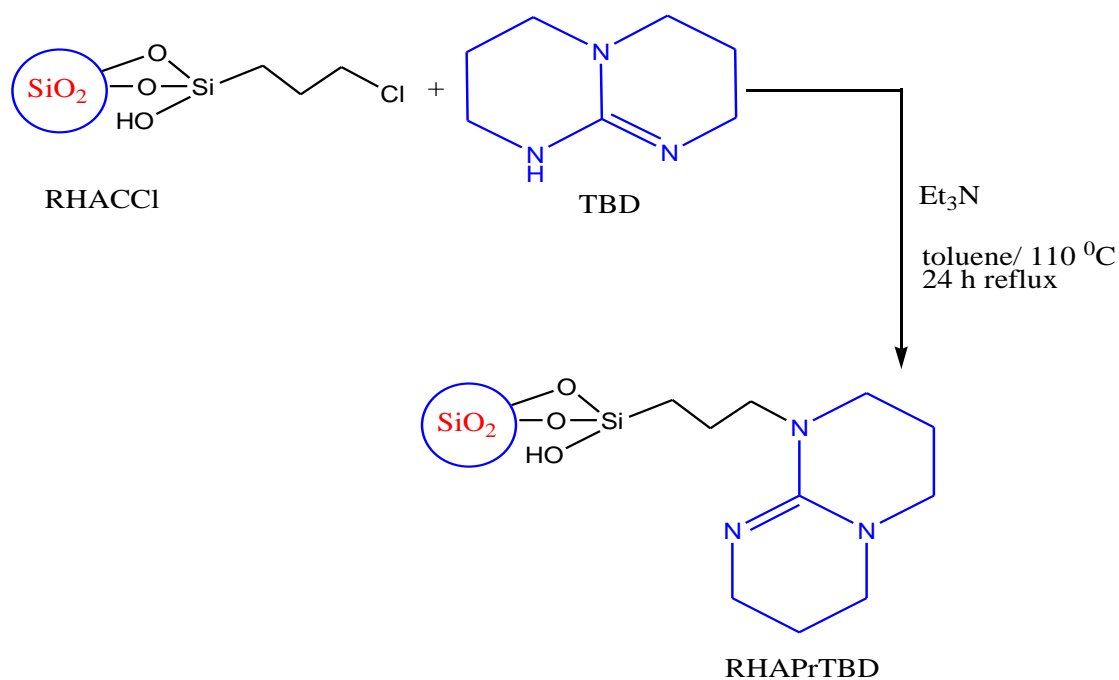
The Michael addition reaction is among the methods of forming a variety of C-C bonds. The conjugate addition of nitroalkane to enoles is a good example of Michael addition reaction. Many reports have shown the successful addition of nitroalkanes to alpha, beta, unsaturated ketones, yielding variety of important products. In this work, the addition reaction of nitro methane with cyclopentenone in presence of TBD as heterogeneous catalyst was studied.

II. Materials and Method

All chemicals used in this study are of high purity and used without further purification.

Preparation of silica-triazabicyclo decene (RHAPrTBD) as catalyst

In the preparation, the method of Farook and Muazu (2013) was followed. A 3.5 mL (27.89 mmol) of 1,5,7-triazabicyclo[4.4.0]dec-5-ene was added to a suspension of modified silica (1.0 g) in unhydrous toluene (30 mL) and triethylamine 3.9 mL (27.89 mmol) as deprotonating agent. The reaction mixture was refluxed at 110 °C in an oil bath for 24 h, under nitrogen atmosphere. The solid product was filtered off, washed with toluene and finally with distilled water. It was dried at 100 °C for 24 h in vacuum, to afford RHAPrTBD catalyst. The synthesis of RHAPrTBD is shown in scheme 1.



Scheme 1: The functionalisation of modified silica with 1,5,7-triazabicyclo[4.4.0] dec-5-ene to form RHAPrTBD catalyst. Et₃N represents triethyl amine.

Characterisation of silica-triazabicyclo[4.4.0] dec-5-ene

The N₂ adsorption desorption analysis

Fig. 1 shows N₂ adsorption isotherms of RHAPrTBD. The functionalized sample displayed type IV isotherm with a clear hysteresis loop typical of type H2 (Cychosz and Thommes, 2018). This type of hysteresis can be classified as ink bottle-shaped pores due to delayed capillary condensation resulting from cavitation mechanism and pore-blocking effect (Park et al., 2016). Furthermore, the closure of the desorption region occurred at $P/P_0 = 0.4$ which typifies the steepest region on the hysteresis. This is an indication that the materials remained mesoporous before and after the functionalisation. The observed decrease in surface area after functionalisation can be attributed to the presence of functional groups that have potentially occupied some active pores, which consequentially resulted in reduction of the surface area. The effect of the propyl group on the pore size of RHACCl was slight compared with TBD/SiO₂, due to the bigger size of the $-(\text{CH}_2)_3\text{TBD}$ groups. The pore size distribution as can be seen inset.

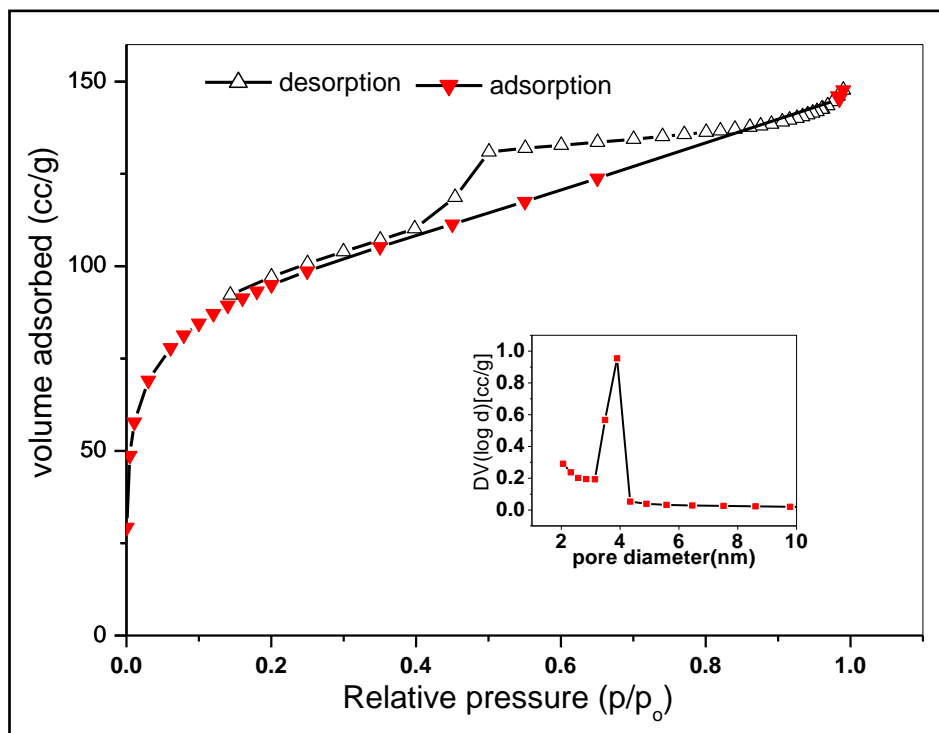


Fig.1: The nitrogen adsorption-desorption isotherm for RHAPrTBD. Inset is the BJH cumulative desorption pore size distribution.

Fourier Transform Infrared Spectroscopy (FT-IR)

Fig. 2 shows the FT-IR spectra of RHA, RHACCI and RHAPrTBD catalyst. The large broad band between 3442 and 3413 cm^{-1} in both RHACCI and RHAPrTBD are both associated with O-H stretching frequency of silanol groups and possibly adsorbed water. The C-H stretching vibration of RHACCI and RHAPrTBD are represented at 2967 cm^{-1} . The absorption band common at 1636 cm^{-1} in RHACCI and RHAPrTBD were also ascribed to angular vibrations of water molecule. The peak at 1528 cm^{-1} in RHAPrTBD represents C=N stretching vibration, while the band at 1442 cm^{-1} is due to N-H bending vibrations (Blanc, et al., 2000, Faria, 2008). The band at 1325 cm^{-1} in RHAPrTBD could be due to C-N stretching vibration. The strong absorption band around 1085 cm^{-1} is due to asymmetric stretching vibration of the structural siloxane bond, Si-O-Si. This peak shifted towards lower wave number for RHAPrTBD, obviously due to the modification of the propyl silica network in RHACCI. The band at 792 cm^{-1} is attributed to Si-O-Si symmetric stretching vibration, while the band at 465 cm^{-1} is due to Si-O-Si bending vibrations (Lenza and Vasconcelos, 2001)

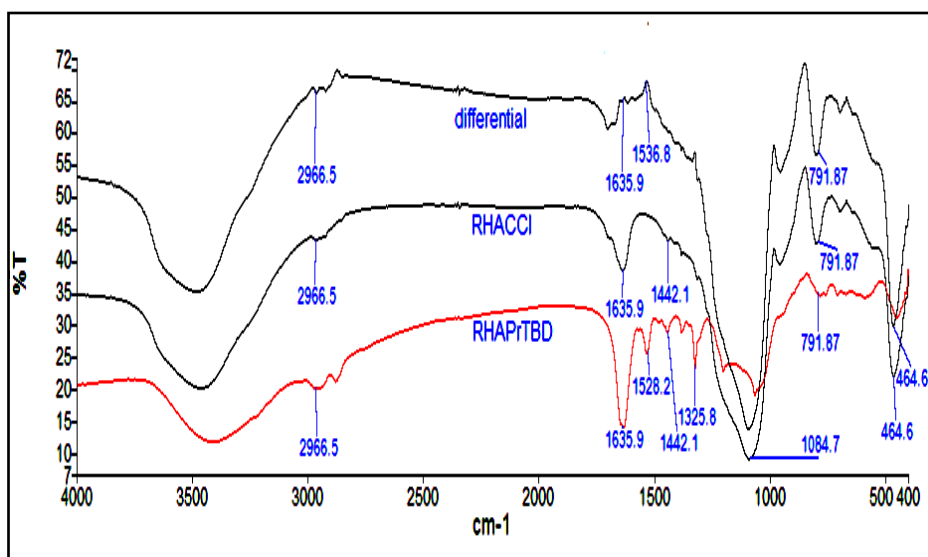


Fig. 2.2: The FT IR spectra of RHACCI, RHAPrTBD and the differential.

The ^{13}C CP/MAS NMR spectroscopy

The solid NMR provides important information about immobilization of pendant groups on the inorganic structure of the catalyst. Figure 5 shows the ^{13}C MAS NMR spectra of RHAPrTBD. The spectrum is consistent with chemical modifications of the silica surface with RHACCl and the catalyst. A series of chemical shifts in the range of 0.60–151 ppm appeared, showing adequately formed peaks. The first two distinct signal peaks observed at $\delta = 0.6$ and 9.7 ppm were assigned to C1 and C2 atoms of the propyl chain attached to the silica network (scheme 2). The characteristic peaks, viz; C3, C4 ($\delta = 20$ ppm); C5 ($\delta = 25$ ppm); C6, C7 ($\delta = 47$ ppm) and C8 ($\delta = 38$ ppm) were also observed. The effect of lone pair on the nitrogen atom, shifted the signal of C9 slightly down field ($\delta = 64$ ppm). The last carbon atom, labelled as C10, appeared at down field, this was due to the presence of pi electrons on the C=N bond, which caused the carbon atom to be de-shielded and therefore appeared at down field position ($\delta = 151$ ppm). The presence of these peaks further confirmed the immobilisation of the guanidine molecule on the silica support.

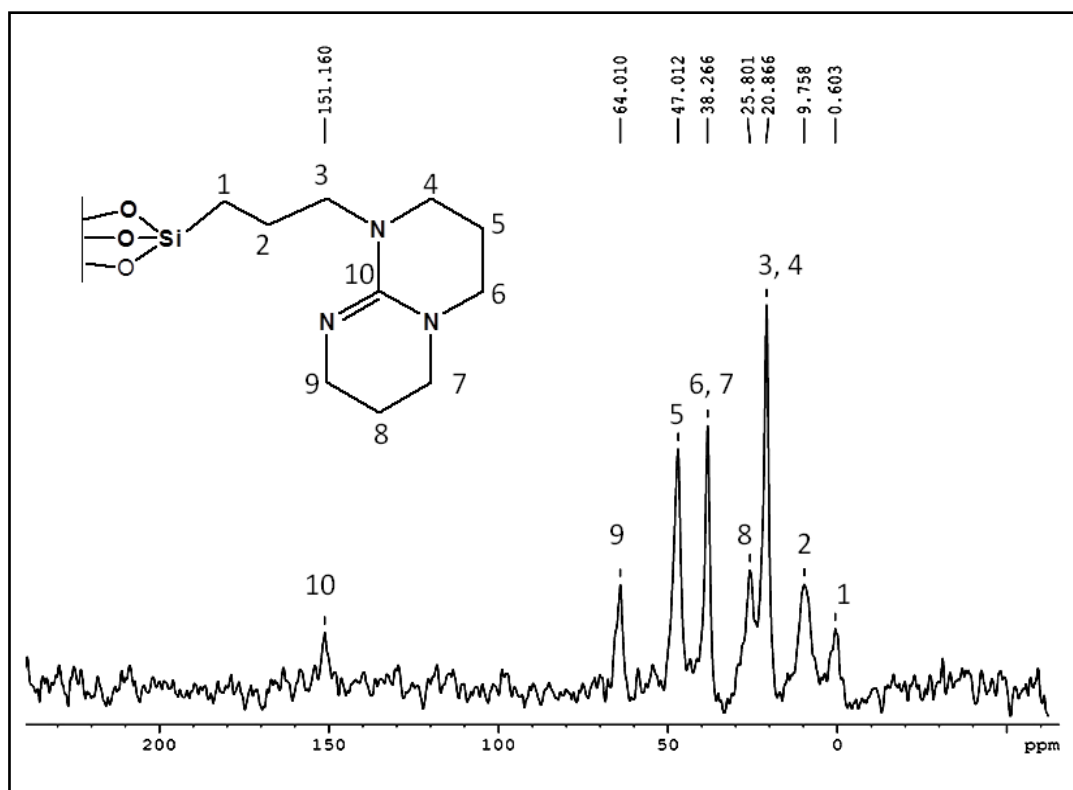


Fig.5: The solid state ^{13}C CP/MAS NMR for RHAPrTBD showing the chemical shift for the various carbon atoms present in the structure.

The Thermo gravimetric / differential thermal analyses (TGA/DTA)

A small amount of the catalyst, RHAPrTBD (10.01 mg) was used to study the thermal analysis (DTA) (Fig.6). The TGA analysis showed three characteristic decomposition stages: the first, starting from 29–139 °C is attributed to loss of water (ca. 5.44 %); the second mass loss (16.47 %, 1.06 mg) occurred from 220 - 415 °C, is due to decomposition of TBD organics from the silica surface. According to this mass loss, 1.20 mmol g^{-1} of TBD was loaded on the silica support (Adam et al., 2010). The third continuous mass loss of ca. 12.05 % occurred between 400 and 750 °C, this was attributed to the dehydration of entrapped water molecules within the silica network and the loss of water due to formation of siloxane bonds through the condensation of neighbouring silanol groups (Adam et al., 2011(a)). Thus, the TGA–DTA data provided further evidence for the successful immobilisation of TBD on the RHACCl to form RHAPrTBD.

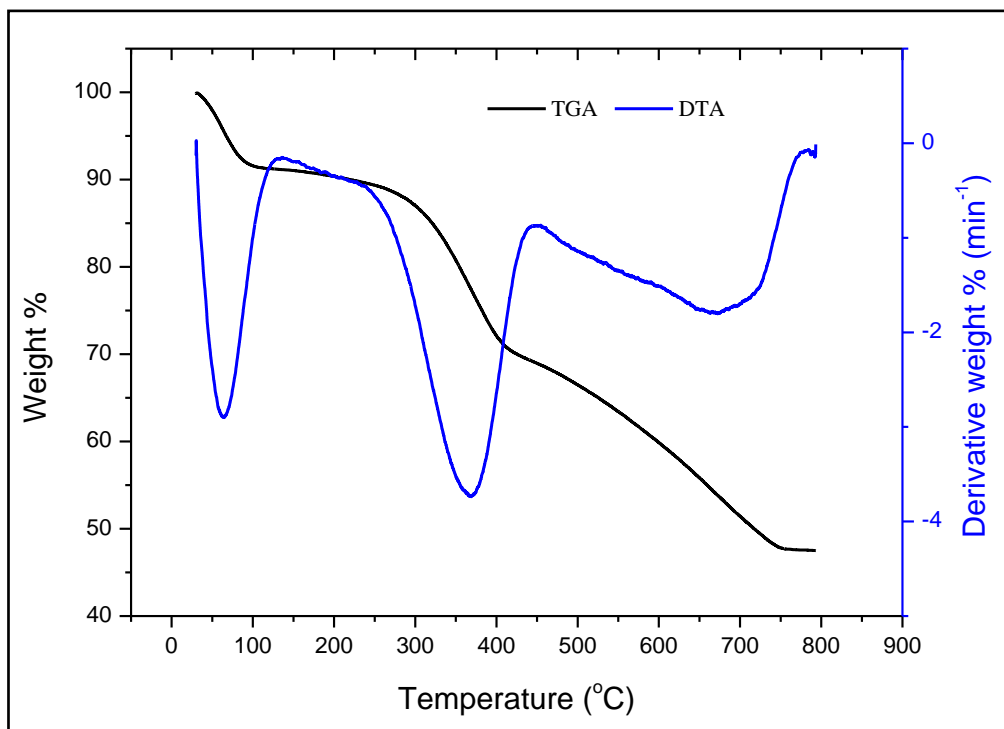


Fig. 6: Thermo gravimetric analysis (TGA) /Differential thermal analysis (DTA) of RHAPrTBD catalyst.

The Electron micrographs (SEM and TEM)

The scanning electron and transmission electron microscopy techniques were used to identify the surface morphology of the samples. Before being scanned with the electronic microscope, the thin powdered sample was first mounted on to an SEM specimen stub with double-sided sticky tape. The specimen was coated with gold and left to dry for about 10–20 min prior to analysis; the scanning electron micrographs at 20 k magnifications are shown in Fig. 8. The SEM picture of the material did not clearly show the particles, however, the only conclusion could be that the samples consist of aggregate particles without regular shape. Thus, confirming the formation of agglomerates.

The transmission electron micrographs (TEM) for RHAPrTBD are shown in Fig. 9. The high degree of homogeneity of the catalyst shows that it is granular and porous. The particles of various sizes were spherical in shape and porous in nature. The spherical shape could be due to the presence of amine group acting as template during the syntheses (Adam and Andas, 2007). Detailed analysis of the particle size was not possible due to their overlap.

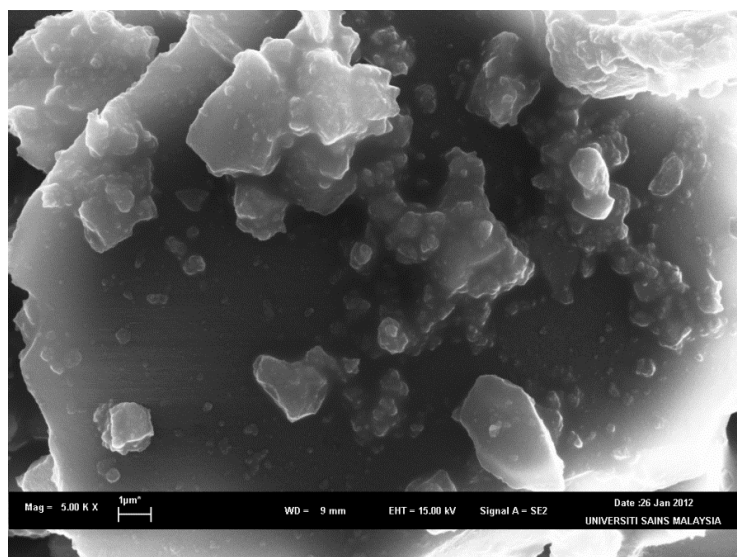


Fig.8: The Scan Electron Microscopy (SEM) image of RHAPrTBD at 20 k magnification.

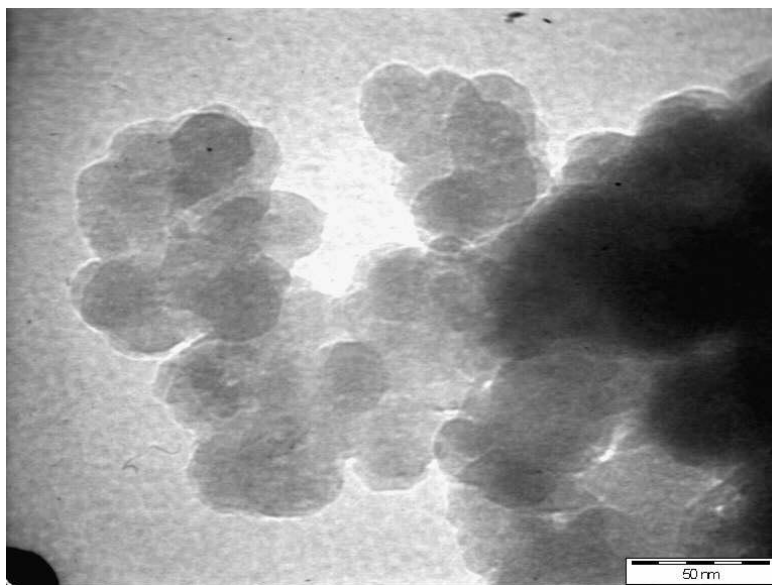


Fig. 9: The Transmission Electron Microscopy (TEM) image of RHAPrTBD, at 260 k magnification.

Reaction of nitromethane with cyclopentenone (Michael Addition reaction)

The reaction was run in a two necked round bottom flask fitted with condenser and magnetic stirrer. 0.3 ml (3.6 mmol) of cyclopentenone and 0.2ml (3.7mmol) of nitromethane in the presence of pre-treated catalyst (0.5g) in ethanol solution was stirred at pre-determined time and temperature. At the end of the reaction, the catalyst was filtered washed and dried for re-run. Gas chromatographic (GC) analyses were performed using GC- Clarus 500, Perkin Elmer, equipped with a flame ionization detector (FID) and a capillary wax column (length=30 m, inner diameter = 0.25 mm and film thickness = 0.25 μm). The GCMS was obtained using Clarus 600, Perkin Elmer to identify the product.

Effect of reaction temperature

The effect of temperature on the reaction of Nitromethane with cyclopentenone was studied and analysed. The result of the conversion and selectivity of the nitromethanecyclopentenone is shown below.

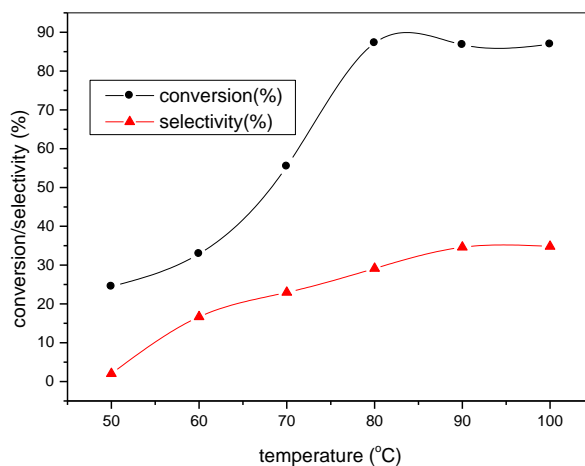


Figure 1: The effect of temperature on the conversion of nitromethane to nitrocyclopentenone parameters kept constant. (catalyst=0.2g, 3.6 mmol of cyclopentenone and 3.7mmol of nitromethane, speed of stirrer=500rpm and reaction time of 6h).

Result above showed that, as temperature increases, both conversion and selectivity increases from 25 to 85% and 2.5 to 25% respectively. It is also evident that the conversion reached optimum above 80 $^{\circ}\text{C}$ which indicated the optimum temperature for the reaction.

Effect of reaction time

Figure 2 shows the effect of time on the conversion of nitromethane towards the selectivity of cyclopentenone. The results indicated that, about 90% conversion was achieved within 3 1/2 hours of the reaction, even though the selectivity towards cyclopentenone was significantly low, accounting for about 5% at the highest conversion. Further reaction at increased reaction time up to 8 hrs shows increased nitromethanecyclopentenone selectivity of 18%. The gradual increase of nitromethanecyclopentenone selectivity from 3 to 18% as time increased from 2 to 8 hrs suggests that the reaction is extremely slow and/or potentially inhibited by the formation of secondary products, since conversion remains high at all reaction times.

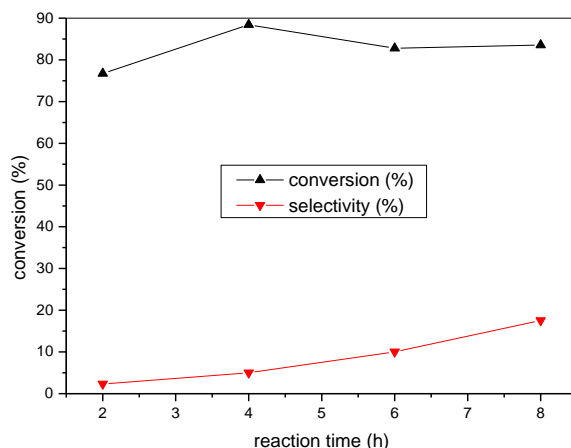


Figure 2: The effect of reaction time on the conversion of nitromethane to nitrocyclopentenone. (catalyst=0.2g, 3.6 mmol of cyclopentenone and 3.7mmol of nitromethane, speed of stirrer=500rpm and temperature=80°C)

The effect of catalyst loading

Figure 3 shows the effect of catalyst loading on the reaction of nitromethane with cyclopentenone. The results showed that, an optimum of about 15 mg of the catalyst is sufficient to give maximum conversion (90%), further addition of the catalyst decreases the conversion significantly.

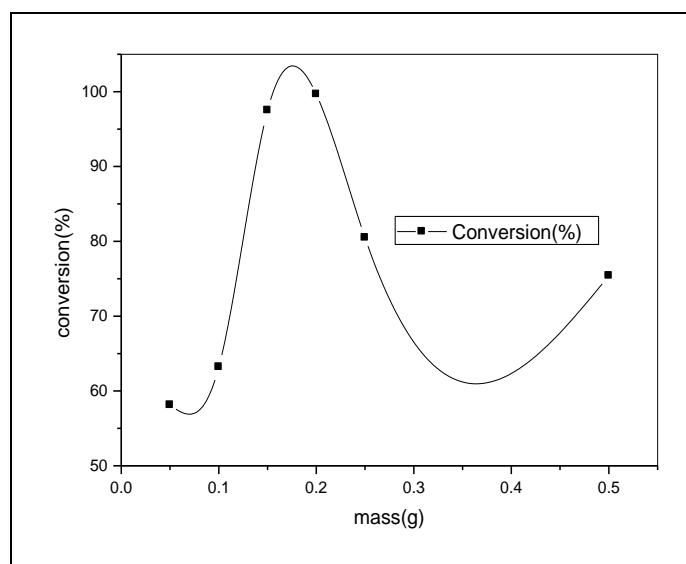


Figure 3: The effect of catalyst loading on the conversion of nitromethane to cyclopentenone nitrocyclopentenone. (3.6 mmol of cyclopentenone and 3.7mmol of nitromethane, speed of stirrer=500rpm and temperature=80°C, time=4h)

Effect of stirrer speed

To ensure a reaction is under kinetic control and not influenced by mass transfer resistances, the extent of liquid phase and liquid-solid mass transfer resistances can be evaluated by the extent of liquid phase agitation on conversion or reaction rates (Zhang et al., 2002). Therefore, this effect is investigated by altering the stirring

speed over a range of 100 to 600 rpm. Figure 4 below shows that the conversion strongly depends on stirring speed between 100 and 300 rpm at which conversion increased from 47% to 87%. At increased stirring speed between 300 to 600 rpm, the conversion became invariant within experimental error. This suggests that the reaction was influenced by external mass transfer between 100 to 300 rpm and subsequently becomes independent of speed between 300 to 600 rpm. The minimum stirring speed of 300 rpm at which no practical change occurred can be regarded as the optimum speed required to achieve a region free of external mass transfer limitation (Lawal et al., 2019). Subsequently, an optimum conversion of 90% was attained in this region. In addition, the minimum speed (300 rpm) is expected to provide the complete suspension of the silica particles which in turn enhances surface reaction and pore diffusion.

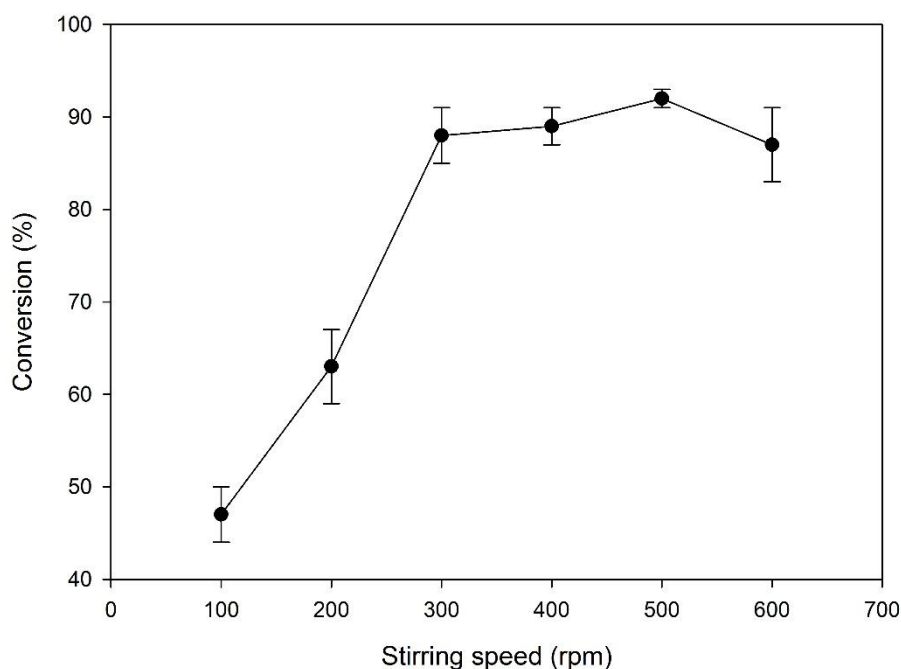


Figure 4: The effect of stirrer speed on the conversion of nitromethane to cyclopentenone nitrocyclopentenone. (catalyst, 0.2g, 3.6 mmol of cyclopentenone and 3.7mmol of nitromethane, temperature=80°C, time=4h)

Reusability study

A series of catalytic cycles were run to investigate the stability of RHAPrTBD. In each case, the catalyst was recovered by separating it from the reaction mixture by centrifuge. It was then followed by rinsing with acetone, dried at 110 °C for 3 h and reused for subsequent reaction. In each cycle, the reaction was performed under the optimized conditions. The results are summarized in Figure 5. It is worth noting that even though there was a slight decrease in conversion from 90 to 87% between the 1st and 2nd reuse, the drop was marginally within 3%. Subsequent re-use showed drastic drop in conversion to 74% and then 65% between the 3rd and 4th reuse respectively. This trend can be attributed to possible leaching of the active component and shrinkage of pores due to agglomeration. In addition, the shrinkage can be linked to functionalized components occupying the catalyst pore sites and thus decreasing the surface area as earlier reported.

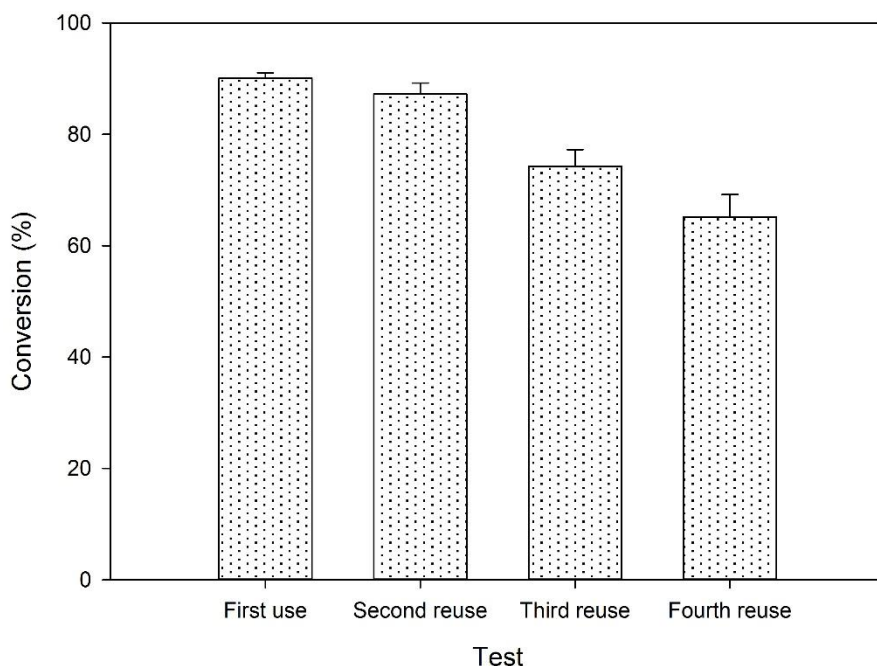


Figure 5. Reusability experiment on the catalyst (3.6 mmol of cyclopentenone and 3.7mmol of nitromethane, temperature=80°C, time=4h, speed of stirrer=500rpm)

III. Conclusion

The article describes a convenient approach to the preparation of triazabicycloguanidine covalently bonded to silica material to obtain a heterogeneous base catalyst was applied in the Michael addition reaction of nitromethane and cyclopentanone. In the literature, the kinetic studies carried out from the reaction of cyclohexenone and nitromethane using TBD catalyst showed that the reaction reached the equilibrium at 3h with a yield of 98% under almost equimolar conditions, similarly, the reaction between cyclohexenone and nitromethane required excess of nitromethane, a temperature of 90 °C and a reaction time of 20 h using propylamines supported on silica as catalyst. In this protocol, we report the reaction of cyclopentenone with the same nitromethane and achieved maximum conversion of 90 % in 4 hours. The catalyst was recycled four more times with excellent conversion for each cycle.

Reference

- [1]. Adam, F., and Andas, J., (2007). Amino benzoic acid modified silica—An improved catalyst for the mono-substituted product in the benzylation of toluene with benzyl chloride. *J. Colloid Interf. Sci.*, 311(1), 135-143.
- [2]. Adam, F., Hello, K.M., Ali, T.A., (2011). Solvent free liquid-phase of phenol over solid sulfanilic acid catalyst, *Appl. Catal. A*, 399, 42-49. Babarini, A., Maggi, R., Mazzachani, A., Mori, G., Sartori, G., and Sartorio R., (2003). Cycloaddition of CO₂ over both homogeneous and silica-supported guanidine catalyst, *Tetrahedron Lett.*, 44, 2931-2934.
- [3]. Barcelo, G., Grenoillat, D., Senet, J.P., and Sennyey, G., (1990). Pentaalkylguanidines as etherification and esterification catalysts, *Tetrahedron*, 46, (6), 1839-1848.
- [4]. Barton, D.H.R., Elliott, J.D., and Gero, S.D. (1982). Synthesis and properties of a series of sterically hindered guanidine bases, *J. Chem. Soc. – Perkin Trans. 1*, 2085–2090.
- [5]. Cychoz, K.A., Thommes, M., 2018. Progress in the Physisorption Characterization of Nanoporous Gas Storage Materials. *Engineering* 4, 559–566.
- [6]. Dai, W.L., Luo, S.L., Yin, S.F., and Au, C.T., (2009). The direct transformation of carbon dioxide to organic carbonates over heterogeneous catalysts, *Appl. Catal. A*, 366, 2-12.
- [7]. de Assunção, L. R., Marinho, E. R., and Proença, F. P., (2010). Guanidine: studies on the reaction with ethyl N-(2-amino-1, 2-dicyanovinyl)formimidate. *ARKIVOC(v)*, 82-91.
- [8]. Farook, A. and Muazu S. B. (2013). Tetramethylguanidine–silica nanoparticles as an efficient and reusable catalyst for the synthesis of cyclic propylene carbonate from carbon dioxide and propylene oxide, *Applied Catalysis A General* 454, 164-171.
- [9]. Faria, E.A., Ramalho, H.F., Marques, J.S., Suarez, P.A.Z., and Prado, A.G.S., (2008). Tetramethylguanidine covalently bonded onto silica gel surface as an efficient and reusable catalyst for transesterification of vegetable oil, *Appl. Catal. A* 338, 72-78.
- [10]. Jérôme, F., Kharchafi, G., Adam, I., and Barrault, J., (2004). “One-pot” and selective synthesis of monoglycerides over homogeneous and heterogeneous guanidine catalysts, *Green Chem.*, 6, 72–74.
- [11]. Lawal, A.M., Hart, A., Daly, H., Hardacre, C., Wood, J., 2019. Kinetics of Hydrogenation of Acetic Acid over Supported Platinum Catalyst. *Energy Fuels* 33, 5551–5560.
- [12]. Lenza, R.F.S., Vasconcelos, W.L., (2001). Preparation of silica by sol-gel method using formamide, *Mater. Res.*, 4(3) 189-194.

- [13]. Ma, D., and Cheng, K., (1999). Enantioselective synthesis of functionalized α - amino acids via a chiral guanidine catalyzed Michael addition reaction, *Tetrahedron: Asymmetry* 10(4), 713–719.
- [14]. Meloni, D., Monachi, R., Zeede, Z., Cutrufello, M.G., Fiorilli, S., and Ferino, I., (2011). Transesterification of soybean oil on Guanidine-functionalised SBA-15 catalysts, *Appl. Catal., B: Environ.*, 102, 505-512.
- [15]. Park, Y.-C., Tokiwa, H., Kakinuma, K., Watanabe, M., Uchida, M., (2016). Effects of carbon supports on Pt distribution, ionomer coverage and cathode performance for polymer electrolyte fuel cells. *J. Power Sources* 315, 179–191.
- [16]. Schwesinger, R., (1985). Extremely strong, non-ionic bases: Syntheses and applications, *Chimia*, 39, 269–272.
- [17]. Schuchardt, U., Serchelia, R., and Vargas, R.M., (1998). Transesterification of vegetable oils: A Review, *J. Braz. Chem. Soc.*, 9(1), 199-210.
- [18]. Sercheli, R., Ferreira, A.L., Guerreiro, M.C., Vargas, R.M., Sheldon, R.A., and Schuchardt, U., (1997). Encapsulation of N,N',N''-tricyclohexylguanidine in hydrophobic zeolite Y: Synthesis and catalytic activity, *Tetrahedron Lett.*, 38(8), 1325-1328.
- [19]. Sercheli, R., Vargas, R.M. and Schuchardt, U., (1999). Alkylguanidine-catalyzed heterogeneous transesterification of soybean, *J. Am. Oil Chem. Soc.* 76 (10), 1207-1210.
- [20]. Ye, W., Xu, J., Tan, C.T., and Tan, C.H., (2005). 1,5,7-Triazabicyclo[4.4.0]dec-5-ene (TBD) catalyzed Michael reactions, *Tetrahedron Lett.*, 46(40), 6875-6878.
- [21]. Zhang, X., Zhao, N., Wei, W., and Sun Y., (2006). Chemical fixation of carbon dioxide to propylene carbonate over-amine-functionalised silica catalysts, *Catal. Today*, 115, 102-106.
- [22]. Zhang, Z., Jackson, J.E., Miller, D.J., 2002. Kinetics of Aqueous-Phase Hydrogenation of Lactic Acid to Propylene Glycol. *Ind. Eng. Chem. Res.* 41, 691–696.

Samaila Muazu Batagarawa, and Ahmed Lawal Mashi. "Triazabicyclodecene Guanidine as Efficient and Reusable Solid Catalyst for the Addition of Nitromethane to Cyclo Pentenone." *IOSR Journal of Applied Chemistry (IOSR-JAC)*, 13(3), (2020): pp 20-29.